

Effect of Radiation and Hall Currents on Mixed Convective Heat and Mass Transfer in a Vertical Wavy Channel

K.Sreeranga Vani^{1#}, U. Rajeswara Rao^{#1}, D.R.V.Prasada Rao^{#1}

^{1#}Department of Mathematics, Sri Krishnadevaraya University, Anantapur, A.P., India

ABSTRACT

We investigate the convective heat and mass transfer flow of a viscous electrically conducting fluid in a vertical wavy channel under the influence of an inclined magnetic field with heat generating sources. The walls of the channels are maintained at constant temperature and concentration. The equations governing the flow heat and concentration are solved by employing perturbation technique with a slope δ of the wavy wall. The velocity, temperature and concentration distributions are investigated for a different values of M , m , N , N_1 , β , Sc and α . The rate of heat and mass transfer are numerically evaluated for a different variations of the governing parameters.

Keywords : Hall Effects, Radiation, Heat Sources, Wavy Channel, Inclined Magnetic Field

INTRODUCTION

Coupled heat and mass transfer by natural convection in a fluid-saturated porous medium has attracted considerable attention in recent years due to many important engineering and geophysical applications such as cooling of nuclear fuel in shipping flasks and water filled storage bags, insulation of high temperature gas-cooled reactor vessels, drums containing heat generating chemicals in the earth, thermal energy storage tanks, regeneration heat exchanges containing catalytic reaction.

In recent years, energy and material saving considerations have prompted an expansion of the efforts at producing efficient heat exchanger equipment through augmentation of heat transfer. It has been established that channels with diverging – converging geometries augment the transportation of heat transfer and momentum. As the fluid flows through a tortuous path viz., the dilated – constricted geometry, there will be more intimate contact between them. The flow takes place both axially (primary) and transversely (secondary) with the secondary velocity being towards the axis in the fluid bulk rather than confining within a thin layer as in straight channels. Hence it is advantageous to go for converging-diverging geometries for improving the design of heat transfer equipment. Vajravelu and Nayfeh [30] have investigated the influence of the wall waviness on friction and pressure drop of the generated coquette flow. Vajravelu and Sastry [29] have analyzed the free convection heat transfer in a viscous, incompressible fluid confined between long vertical wavy walls is the presence of constant heat source. Later Vajravelu and Debnath [28] have extended this study to convective flow in a vertical wavy channel in four different geometrical configurations. This problem has been extended to the case of wavy walls by McMichael and Deutsch [13], Deshikachar et al [8] Rao *et. al.*, [16] and Sree Ramachandra Murthy [27]. Hyan Gook Won *et. al.*, [9] have analyzed that the flow and heat/mass transfer in a wavy duct with various corrugation angles in two dimensional flow regimes. Mahdy *et. al.*, [12] have studied the mixed convection heat and mass transfer on a vertical wavy plate

embedded in a saturated porous media (PST/PSE) Comini *et. al.*, [5] have analyzed the convective heat and mass transfer in wavy finned-tube exchangers. Jer-Huan Jang *et. al.*, [10] have analyzed that the mixed convection heat and mass transfer along a vertical wavy surface.

The study of heat and mass transfer from a vertical wavy wall embedded into a porous media became a subject of great interest in the research activity of the last two decades: Rees and Pop studied the free convection process along a vertical wavy channel embedded in a Darcy porous media, a wall that has a constant surface temperature [18] or a constant surface heat flux [19]. Kumar and Gupta [17] for a thermal and mass stratified porous medium and Cheng [4] for a power law fluid saturated porous medium with thermal and mass stratification. The influence of a variable heat flux on natural convection along a corrugated wall in a non-Darcy porous medium was established by Shalini and Kumar [23].

Kumar et al [17] have discussed the time dependent thermal convection of a viscous, electrically conducting fluid through a porous medium in horizontal channel bounded by wavy walls. Kumar [17] has discussed the two-dimensional heat transfer of a free convective MHD flow with radiation and temperature dependent heat source of a viscous incompressible fluid, in a vertical wavy channel. Recently Mahdy et al [12] have presented the Non-similarity solutions have been presented for the natural convection from a vertical wavy plate embedded in a saturated porous medium in the presence of surface mass transfer.

In all these investigations, the effects of Hall currents are not considered. However, in a partially ionized gas, there occurs a Hall current [6] when the strength of the impressed magnetic field is very strong. These Hall effects play a significant role in determining the flow features. Sato [21], Yamanishi [31], Sherman and Sutton [25] have discussed the Hall effects on the steady hydromagnetic flow between two parallel plates. These effects in the unsteady cases were discussed by Pop [15]. Debnath [7] has studied the effects of Hall currents on unsteady hydromagnetic flow past a porous plate in a rotating fluid system and the structure of the steady and unsteady flow is investigated. Alam *et. al.*, [2] have studied unsteady free convective heat and mass transfer flow in a rotating system with Hall currents, viscous dissipation and Joule heating. Taking Hall effects in to account Krishna *et. al.*, [11] have investigated Hall effects on the unsteady hydromagnetic boundary layer flow. Rao *et. al.*, [16] have analyzed Hall effects on unsteady Hydromagnetic flow. Siva Prasad *et. al.*, [26] have studied Hall effects on unsteady MHD free and forced convection flow in a porous rotating channel. Recently Seth *et. al.*, [22] have investigated the effects of Hall currents on heat transfer in a rotating MHD channel flow in arbitrary conducting walls. Sarkar *et. al.*, [20] have analyzed the effects of mass transfer and rotation and flow past a porous plate in a porous medium with variable suction in slip flow region. Anwar Beg et al [3] have discussed unsteady magnetohydrodynamics Hartmann-Couette flow and heat transfer in a Darcian channel with Hall current, ion slip, Viscous and Joule heating effects. Ahmed [1] has discussed the Hall effects on transient flow past an impulsively started infinite horizontal porous plate in a rotating system. Shanti [24] has investigated effect of Hall current on mixed convective heat and mass transfer flow in a vertical wavy channel with heat sources. Leela [14] has studied the effect of Hall currents on the convective heat and mass transfer flow in a horizontal wavy channel under inclined magnetic field.

In this paper, we investigate the effect of thermal radiation on convective heat and mass transfer flow of a viscous electrically conducting fluid in a vertical wavy channel under the influence of an inclined magnetic fluid with heat generating sources. The walls of the channels are maintained at constant temperature and concentration. The equations governing

the flow heat and mass transfer are solved by employing perturbation technique with the slope δ of the wavy wall as a perturbation parameter. The velocity, temperature and concentration distributions are investigated for different values of G , M , m , N , N_1 , α and x . The rate of heat and mass transfer are numerically evaluated for a different variations of the governing parameters.

FORMULATION AND SOLUTION OF THE PROBLEM

We consider the steady flow of an incompressible, viscous, electrically conducting fluid confined in a vertical channel bounded by two wavy walls under the influence of an inclined magnetic field of intensity H_0 lying in the plane (y-z). The magnetic field is inclined at an angle α_1 to the axial direction k and hence its components are $(0, H_0 \sin(\alpha_1), H_0 \cos(\alpha_1))$. In view of the waviness of the wall the velocity field has components $(u, 0, w)$. The magnetic field in the presence of fluid flow induces the current $(J_x, 0, J_z)$. We choose a rectangular cartesian co-ordinate system $O(x, y, z)$ with z -axis in the vertical direction and the walls at $x = \pm f(\frac{\delta z}{L})$.

When the strength of the magnetic field is very large we include the Hall current so that the generalized Ohm's law is modified to

$$\vec{J} + \omega_e \tau_e \vec{J} \times \vec{H} = \sigma (\vec{E} + \mu_e \vec{q} \times \vec{H}) \quad (1)$$

where \vec{q} is the velocity vector. \vec{H} is the magnetic field intensity vector. \vec{E} is the electric field, \vec{J} is the current density vector, ω_e is the cyclotron frequency, τ_e is the electron collision time, σ is the fluid conductivity and μ_e is the magnetic permeability. Neglecting the electron pressure gradient, ion-slip and thermo-electric effects and assuming the electric field $E=0$, equation (4) reduces

$$j_x - m H_0 J_z \sin(\alpha_1) = -\sigma \mu_e H_0 w \sin(\alpha_1) \quad (2)$$

$$J_z + m H_0 J_x \sin(\alpha_1) = \sigma \mu_e H_0 u \sin(\alpha_1) \quad (3)$$

where $m = \omega_e \tau_e$ is the Hall parameter.

The governing equations in terms of stream function are

$$u \frac{\partial u}{\partial x} + w \frac{\partial u}{\partial z} = -\frac{\partial p}{\partial x} + \mu \left(\frac{\partial^2 u}{\partial x^2} + \frac{\partial^2 u}{\partial z^2} \right) + \mu_e (-H_0 J_z \sin(\alpha_1)) \quad (4)$$

$$u \frac{\partial W}{\partial x} + w \frac{\partial W}{\partial z} = -\frac{\partial p}{\partial z} + \mu \left(\frac{\partial^2 W}{\partial x^2} + \frac{\partial^2 W}{\partial z^2} \right) + \mu_e (H_0 J_x \sin(\alpha_1)) \quad (5)$$

Eliminating the pressure from equations (4) & (5) and introducing the Stokes Stream function ψ as

$$u = -\frac{\partial \psi}{\partial z}, \quad w = \frac{\partial \psi}{\partial x} \quad (6)$$

the equations (2) - (5) in terms of ψ is

$$\begin{aligned} \frac{\partial \psi}{\partial z} \frac{\partial (\nabla^2 \psi)}{\partial x} - \frac{\partial \psi}{\partial x} \frac{\partial (\nabla^2 \psi)}{\partial z} = \mu \nabla^4 \psi + \beta g \frac{\partial (T - T_e)}{\partial x} \beta^* g \frac{\partial (C - C_e)}{\partial x} - \\ - \left(\frac{\sigma \mu_e^2 H_0^2 \sin^2(\alpha_1)}{1 + m^2 H_0^2 \sin^2(\alpha_1)} \right) \nabla^2 \psi \end{aligned} \quad (7)$$

$$\rho C_p \left(\frac{\partial \psi}{\partial x} \frac{\partial T}{\partial z} - \frac{\partial \psi}{\partial z} \frac{\partial T}{\partial x} \right) = k_f \left(\frac{\partial^2 T}{\partial x^2} + \frac{\partial^2 T}{\partial z^2} \right) + Q(T_e - T) + \frac{16\sigma^* T_e^3}{3\beta_R} \frac{\partial^2 T}{\partial x^2} \quad (8)$$

$$\left(\frac{\partial \psi}{\partial x} \frac{\partial C}{\partial z} - \frac{\partial \psi}{\partial z} \frac{\partial C}{\partial x} \right) = D_1 \left(\frac{\partial^2 C}{\partial x^2} + \frac{\partial^2 C}{\partial z^2} \right) \quad (9)$$

The boundary conditions are

$$u=0, w=0, T=T_1, C=C_1 \text{ on } x = -f\left(\frac{\delta z}{L}\right) \quad (10)$$

$$w=0, u=0, T=T_2, C=C_2 \text{ on } x = f\left(\frac{\delta z}{L}\right) \quad (11)$$

With the flow is maintained by a constant volume flux for which a characteristic velocity is defined as

$$q = \frac{1}{L} \int_{-L_f}^{L_f} w dx \quad (12)$$

$$\text{where } u = -\frac{\partial \psi}{\partial z}, \quad w = \frac{\partial \psi}{\partial x}.$$

On introducing the following non-dimensional variables

$$(x', z') = (x, z) / L, \psi' = \frac{\psi}{qL}, \theta = \frac{T - T_2}{T_1 - T_2}, C' = \frac{C - C_2}{C_1 - C_2}$$

the equation of momentum and energy in the non-dimensional form are

$$\nabla^4 \psi - M_1^2 \nabla^2 \psi + \frac{G}{R} \left(\frac{\partial \theta}{\partial x} + N \frac{\partial C}{\partial x} \right) = R \left(\frac{\partial \psi}{\partial z} \frac{\partial (\nabla^2 \psi)}{\partial x} - \frac{\partial \psi}{\partial x} \frac{\partial (\nabla^2 \psi)}{\partial z} \right) \quad (13)$$

$$PR \left(\frac{\partial \psi}{\partial x} \frac{\partial \theta}{\partial z} - \frac{\partial \psi}{\partial z} \frac{\partial \theta}{\partial x} \right) = \nabla^2 \theta - \alpha \theta + \frac{4}{3N_1} \frac{\partial^2 \theta}{\partial x^2} \quad (14)$$

$$ScR \left(\frac{\partial \psi}{\partial x} \frac{\partial C}{\partial z} - \frac{\partial \psi}{\partial z} \frac{\partial C}{\partial x} \right) = \nabla^2 C \quad (15)$$

where

$$G = \frac{\beta g \Delta T_e L^3}{\nu^2} \quad (\text{Grashof Number}),$$

$$M^2 = \frac{\sigma \mu_e^2 H_o^2 L^2}{\nu^2} \quad (\text{Hartman Number})$$

$$M_1^2 = \frac{M^2 \sin^2(\alpha_1)}{1 + m^2},$$

$$R = \frac{qL}{\nu} \quad (\text{Reynolds Number})$$

$$P = \frac{\mu C_p}{K_f} \quad (\text{Prandtl Number}),$$

$$\alpha = \frac{QL^2}{\Delta TK_f} \quad (\text{Heat Source Parameter})$$

$$Sc = \frac{\nu}{D_1} \quad (\text{Schmidt Number}),$$

$$N = \frac{\beta^* (C_1 - C_2)}{\beta (T_1 - T_2)} \quad (\text{Buoyancy ratio})$$

$$N_1 = \frac{3\beta_R K_f}{4\sigma^* T_e^3} \quad (\text{Radiation parameter}),$$

$$N_2 = \frac{3N_1}{3N_1 + 4} \quad \alpha_2 = \alpha N_2 \quad P_1 = P N_2$$

The corresponding boundary conditions are

$$\begin{aligned}\psi(f) - \psi(-f) &= 1 \\ \frac{\partial \psi}{\partial z} &= 0, \frac{\partial \psi}{\partial x} = 0, \theta = 1, C = 1 \quad \text{at } x = -f(\delta z) \\ \frac{\partial \psi}{\partial z} &= 0, \frac{\partial \psi}{\partial x} = 0, \theta = 0, C = 0 \quad \text{at } x = +f(\delta z)\end{aligned}$$

ANALYSIS OF THE FLOW

Introduce the transformation such that

$$\bar{z} = \delta z, \frac{\partial}{\partial z} = \delta \frac{\partial}{\partial \bar{z}}$$

$$\text{Then } \frac{\partial}{\partial z} \approx O(\delta) \rightarrow \frac{\partial}{\partial \bar{z}} \approx O(1)$$

For small values of $\delta \ll 1$, the flow develops slowly with axial gradient of order δ and hence we take $\frac{\partial}{\partial \bar{z}} \approx O(1)$.

Using the above transformation the equations (13)-(15) reduce to

$$F^4 \psi - M_1^2 F^2 \psi + \frac{G}{R} \left(\frac{\partial \theta}{\partial x} + N \frac{\partial C}{\partial x} \right) = \delta R \left(\frac{\partial \psi}{\partial \bar{z}} \frac{\partial (F^2 \psi)}{\partial x} - \frac{\partial \psi}{\partial x} \frac{\partial (F^2 \psi)}{\partial \bar{z}} \right) \quad (16)$$

$$\delta P_1 R \left(\frac{\partial \psi}{\partial x} \frac{\partial \theta}{\partial \bar{z}} - \frac{\partial \psi}{\partial \bar{z}} \frac{\partial \theta}{\partial x} \right) = F^2 \theta - \alpha_2 \theta \quad (17)$$

$$\delta S c R \left(\frac{\partial \psi}{\partial x} \frac{\partial C}{\partial \bar{z}} - \frac{\partial \psi}{\partial \bar{z}} \frac{\partial C}{\partial x} \right) = F^2 C \quad (18)$$

where

$$F^2 = \frac{\partial}{\partial x^2} + \delta^2 \frac{\partial}{\partial \bar{z}^2}, \quad P_1 = \frac{3N_1 P}{3N_1 + 4}, \quad \alpha_2 = \frac{3N_1 \alpha}{3N_1 + 4}$$

Assuming the slope δ of the wavy boundary to be small we take

$$\begin{aligned}\psi(x, z) &= \psi_0(x, y) + \delta \psi_1(x, z) + \delta^2 \psi_2(x, z) + \dots \\ \theta(x, z) &= \theta_0(x, z) + \delta \theta_1(x, z) + \delta^2 \theta_2(x, z) + \dots \\ C(x, z) &= C_0(x, z) + \delta C_1(x, z) + \delta^2 C_2(x, z) + \dots\end{aligned} \quad (19)$$

$$\text{Let } \eta = \frac{x}{f(\bar{z})} \quad (20)$$

Substituting (19 & 20) in equations (16) - (18) and equating the like powers of δ the equations and the respective boundary conditions to the zeroth order are

$$\frac{\partial^2 \theta_0}{\partial \eta^2} - (\alpha_2 f^2) \theta_0 = 0 \quad (21)$$

$$\frac{\partial^2 C_0}{\partial \eta^2} = 0 \quad (22)$$

$$\frac{\partial^4 \psi_0}{\partial \eta^4} - (M_1^2 f^2) \frac{\partial^2 \psi_0}{\partial \eta^2} = -\frac{G f^3}{R} \left(\frac{\partial \theta_0}{\partial \eta} + N \frac{\partial C_0}{\partial \eta} \right) \quad (23)$$

with

$$\left. \begin{aligned} \psi_0(+1) - \psi_0(-1) &= 1 \\ \frac{\partial \psi_0}{\partial \eta} &= 0, \quad \frac{\partial \psi_0}{\partial \bar{z}} = 0, \quad \theta_0 = 1, \quad C_0 = 1 \quad \text{at } \eta = -1 \\ \frac{\partial \psi_0}{\partial \eta} &= 0, \quad \frac{\partial \psi_0}{\partial \bar{z}} = 0, \quad \theta_0 = 0, \quad C_0 = 0 \quad \text{at } \eta = +1 \end{aligned} \right| \quad (24)$$

and to the first order are

$$\frac{\partial^2 \theta_1}{\partial \eta^2} - (\alpha_2 f^2) \theta_1 = P_1 Rf \left(\frac{\partial \psi_0}{\partial \eta} \frac{\partial \theta_0}{\partial \bar{z}} - \frac{\partial \psi_0}{\partial \bar{z}} \frac{\partial \theta_0}{\partial \eta} \right) \quad (25)$$

$$\frac{\partial^2 C_1}{\partial \eta^2} = Sc Rf \left(\frac{\partial \psi_0}{\partial \eta} \frac{\partial C_0}{\partial \bar{z}} - \frac{\partial \psi_0}{\partial \bar{z}} \frac{\partial C_0}{\partial \eta} \right) \quad (26)$$

$$\left. \begin{aligned} \frac{\partial^4 \psi_1}{\partial \eta^4} - (M_1^2 f^2) \frac{\partial^2 \psi_1}{\partial \eta^2} &= -\frac{Gf^3}{R} \left(\frac{\partial \theta_1}{\partial \eta} + N \frac{\partial C_1}{\partial \eta} \right) + \\ &Rf \left(\frac{\partial \psi_0}{\partial \eta} \frac{\partial^3 \psi_0}{\partial \bar{z}^3} - \frac{\partial \psi_0}{\partial \bar{z}} \frac{\partial^3 \psi_0}{\partial x \partial \bar{z}^2} \right) \end{aligned} \right| \quad (27)$$

with

$$\left. \begin{aligned} \psi_1(+1) - \psi_1(-1) &= 0 \\ \frac{\partial \psi_1}{\partial \eta} &= 0, \quad \frac{\partial \psi_1}{\partial \bar{z}} = 0, \quad \theta_1 = 0, \quad C_1 = 0 \quad \text{at } \eta = -1 \\ \frac{\partial \psi_1}{\partial \eta} &= 0, \quad \frac{\partial \psi_1}{\partial \bar{z}} = 0, \quad \theta_1 = 0, \quad C_1 = 0 \quad \text{at } \eta = +1 \end{aligned} \right| \quad (28)$$

The equation (21) – (23), (25) – (27) are solved analytically subject to the boundary conditions (24) & (28).

NUSSELT NUMBER and SHERWOOD NUMBER

The rate of heat transfer (Nusselt Number) on the walls has been calculated using the formula

$$Nu = \frac{1}{f(\theta_m - \theta_w)} \left(\frac{\partial \theta}{\partial \eta} \right)_{\eta=\pm 1}$$

where $\theta_m = 0.5 \int_{-1}^1 \theta d\eta$

$$(Nu)_{\eta=+1} = \frac{1}{f\theta_m} (a_{78} + \delta(a_{76} + a_{77})), \quad (Nu)_{\eta=-1} = \frac{1}{f(\theta_m - 1)} (a_{79} + \delta(a_{77} - a_{76}))$$

$$\theta_m = a_{80} + \delta a_{81}$$

The rate of mass transfer (Sherwood Number) on the walls has been calculated using the formula

$$Sh = \frac{1}{f(C_m - C_w)} \left(\frac{\partial C}{\partial \eta} \right)_{\eta=\pm 1} \quad \text{where} \quad C_m = 0.5 \int_{-1}^1 C d\eta$$

$$(Sh)_{\eta=+1} = \frac{1}{fC_m} (a_{74} + \delta a_{70}),$$

$$(Sh)_{\eta=-1} = \frac{1}{f(C_m - 1)} (a_{75} + \delta a_{71})$$

$C_m = a_{73} + \delta a_{72}$, where $a_{71} - a_{79}$ are constants involving the parameters.

RESULTS AND DISCUSSION OF THE NUMERICAL RESULTS

In this analysis we discuss the effect of Hall currents and thermal radiation on mixed convective heat and mass transfer flow in a vertical wavy channel under the influence of an inclined magnetic field. The non-linear coupled equations governing the flow, heat and mass transfer are solved by a regular perturbation technique with δ the slope of the wavy wall as a perturbation parameter.

The axial velocity (u) is shown in Figs (1-4) for different values of $M, m, \alpha, N, Sc, \beta$ and N_1 . Fig (1) represents the variation of w with M and m it is found that higher the Lorentz force smaller $|u|$ in the flow region. Thus the magnetic field retards the magnitude of the axial velocity in the flow region. An increase in the Hall parameter m results an enhancement in the axial velocity. Fig (2) represents the variation of w with buoyancy ratio N and heat source parameter α with respect to N we find that when the molecular buoyancy force dominates over the thermal buoyancy force. The axial velocity enhances when the buoyancy force act in the same direction and for the forces act in the opposite direction the axial velocity depreciates in the flow region. The variation of u with α shows that higher the strength of the heat generating sources smaller the velocity u in the entire flow region. Fig (3) represents the variation of u with Sc and β it is found that lesser the molecular diffusivity larger the velocity u also higher the constriction of the channel walls larger u in the region. Thus the wavyness of the boundaries results in an enhancement in the axial velocity. The effect of thermal radiation (N_1) on u is exhibited in fig(4). It is found that higher the radiative heat flux lesser u in the entire flow region. Moving along the axial direction of the channel walls the axial velocity depreciates with axial distance x in the entire flow region fixing the other parameters.

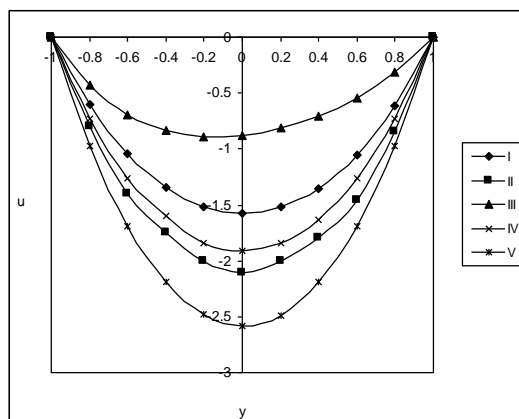


Fig. 1 : Variation of u with M & m

	I	II	III	IV	V
M	2	4	6	2	2
α	0.5	0.5	0.5	1.5	2.5

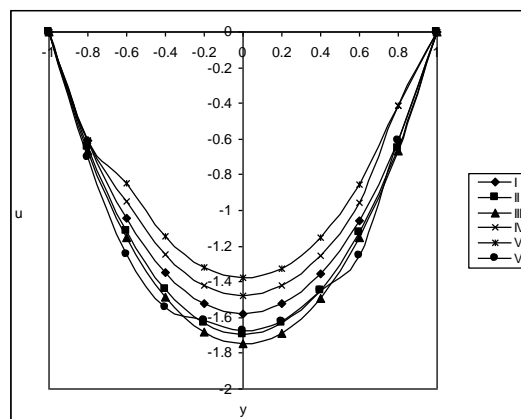


Fig. 2: Variation of u with α & N

	I	II	III	IV	V	VI
α	2	4	6	2	2	2
N	1	1	1	2	-0.5	-0.8

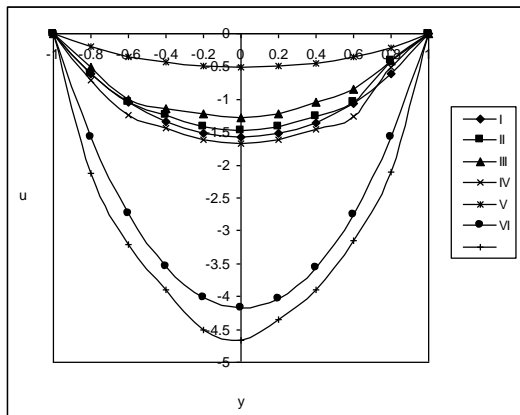


Fig. 3 : Variation of u with Sc & β

	I	II	III	IV	V	VI	VII
Sc	0.24	0.6	1.3	2.01	1.3	1.3	1.3
β	-0.5	-0.5	-0.5	-0.5	-0.3	-0.7	-0.9

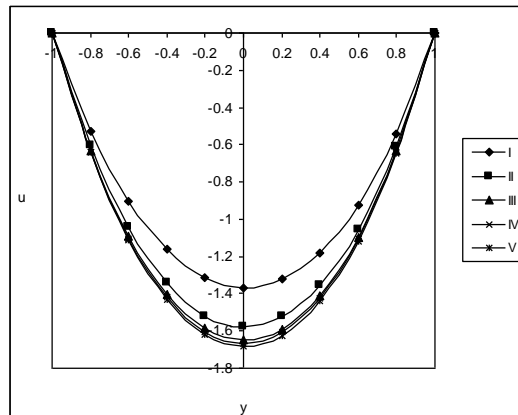


Fig. 4: Variation of u with N_1

	I	II	III	IV	V	VI
N_1	0.5	1.5	3.5	5	10	100

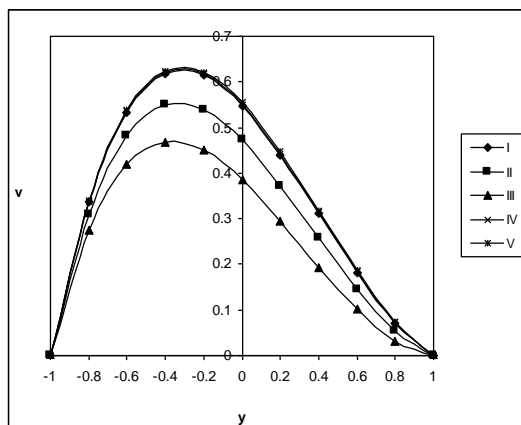


Fig. 5 : Variation of v with M & m

	I	II	III	IV	V
M	2	4	6	2	2
α	0.5	0.5	0.5	1.5	2.5

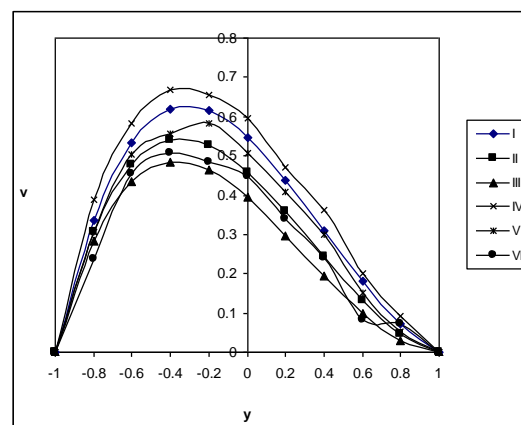


Fig. 6: Variation of v with α & N

	I	II	III	IV	V	VI
α	2	4	6	2	2	2
N	1	1	1	2	-0.5	-0.8

The secondary velocity which is due to the waviness of the boundaries is exhibited in figs (5 – 8) for different parametric variations. The variation of u with M and m is shown in fig (5). It is found that for higher values of $M = 4$ the secondary velocity v changes the direction from towards the mid region to towards the boundary and again at further $M = 6$ it changes the direction again towards the mid region. An increase in the Hall parameter leads to an enhancement in $|u|$. Fig (6) represents the variation of u with N and α it is found that when the molecular buoyancy force dominates over the thermal buoyancy force, $|u|$ depreciates when the molecular buoyancy forces act in the same direction and for the forces act in the opposite direction $|u|$ enhances in the entire region. With respect to α we notice that $|u|$ enhances with increase in the strength of the heat source. From Fig (7) we find that lesser the molecular diffusivity smaller $|u|$ and for further lowering of the diffusivity larger $|u|$. The variation of u with β shows that higher the constriction of the channel walls larger $|u|$ in the entire flow region. From Fig (8) we find that $|u|$ enhances with increase in the radiation parameter N_1 . Thus higher the radiative heat flux larger the magnitude of u in the flow region.

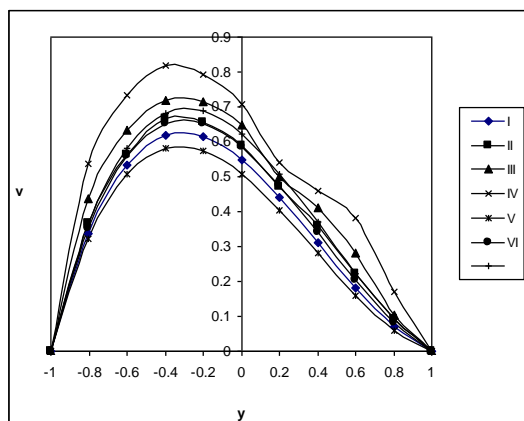


Fig. 7 : Variation of v with Sc & β

	I	II	III	IV	V	VI	VII
Sc	0.24	0.6	1.3	2.01	1.3	1.3	1.3
β	-0.5	-0.5	-0.5	-0.5	-0.3	-0.7	-0.9

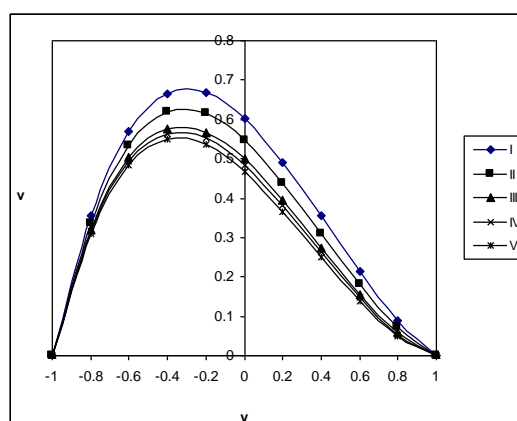


Fig. 8: Variation of v with N_1

	I	II	III	IV	V	VI
N_1	0.5	1.5	3.5	5	10	100

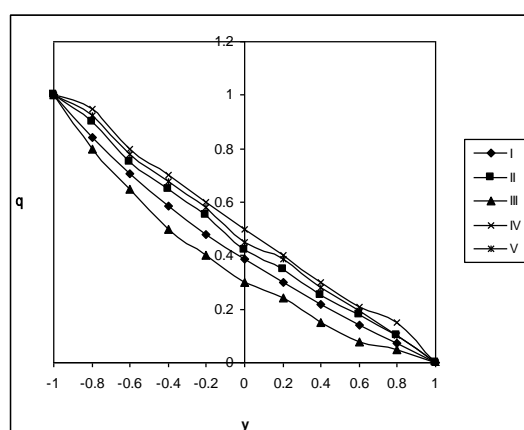


Fig. 9 : Variation of θ with M & m

	I	II	III	IV	V
M	2	4	6	2	2
α	0.5	0.5	0.5	1.5	2.5

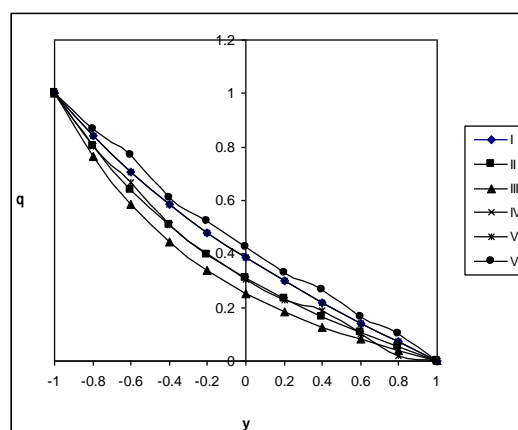


Fig. 10: Variation of θ with α & N

	I	II	III	IV	V	VI
α	2	4	6	2	2	2
N	1	1	1	2	-0.5	-0.8

A non-dimensional temperature θ is shown in figs (9 – 12) for different parametric values. A non-dimensional temperature is positive for all variations. This implies that the actual temperature is always greater than T_2 . Fig (9) represents θ with M and m it is found that the actual temperature enhances with increase in $M \leq 4$ and for further higher $M \geq 6$ we notice an enhancement in θ also an increase in $m \leq 1.5$ results in an enhancement in θ and depreciates for higher $m \geq 2.5$. The variation of θ with N and α is shown in fig (10). With respect to N we find that when the molecular buoyancy force dominates over the thermal buoyancy force the actual temperature enhances irrespective of the directions of the buoyancy forces. Also it reduces to with increase in the strength of the heat source. Fig (11) represents θ with Sc and β . The variation of θ with Sc shows that lesser the molecular diffusivity smaller the actual temperature in the entire flow region. With respect to β we notice that higher the constriction of the channel walls larger the actual temperature in the flow region. From Fig (12) we find that higher the radiative heat flux lesser the actual temperature in the flow region.

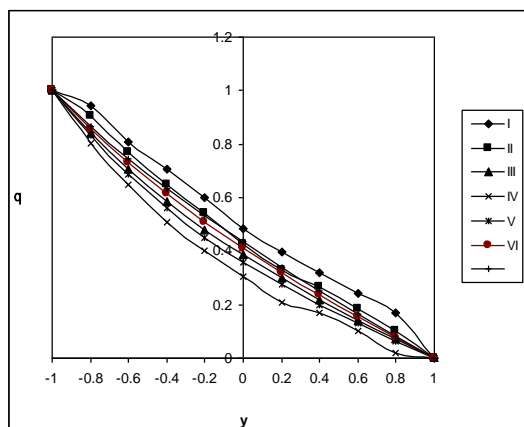


Fig. 11 : Variation of θ with Sc & β

	I	II	III	IV	V	VI	VII
Sc	0.24	0.6	1.3	2.01	1.3	1.3	1.3
β	-0.5	-0.5	-0.5	-0.5	-0.3	-0.7	-0.9

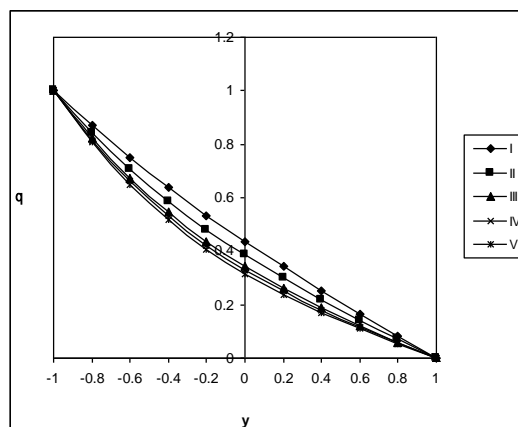


Fig. 12: Variation of θ with N_1

	I	II	III	IV	V	VI
N_1	0.5	1.5	3.5	5	10	100

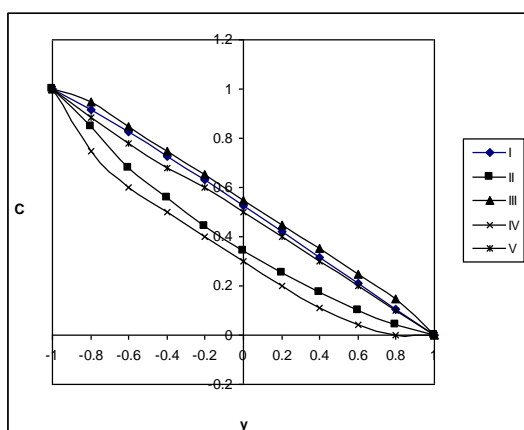


Fig. 13 : Variation of C with M & m

	I	II	III	IV	V
M	2	4	6	2	2
α	0.5	0.5	0.5	1.5	2.5

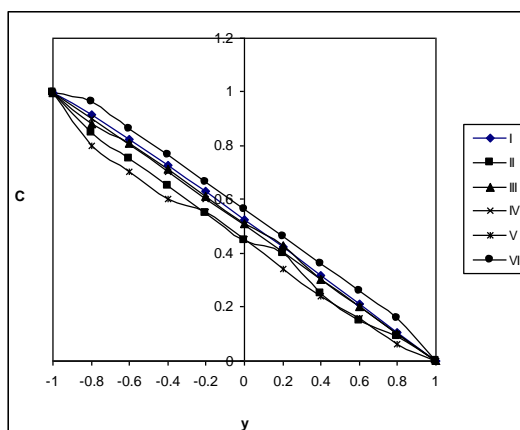


Fig. 14: Variation of C with α & N

	I	II	III	IV	V	VI
α	2	4	6	2	2	2
N	1	1	1	2	-0.5	-0.8

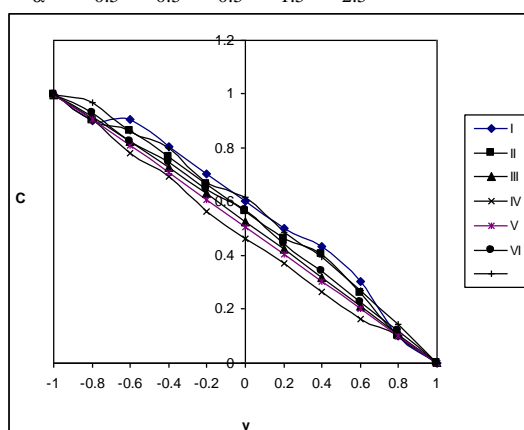


Fig. 15 : Variation of C with Sc & β

	I	II	III	IV	V	VI	VII
Sc	0.24	0.6	1.3	2.01	1.3	1.3	1.3
β	-0.5	-0.5	-0.5	-0.5	-0.3	-0.7	-0.9

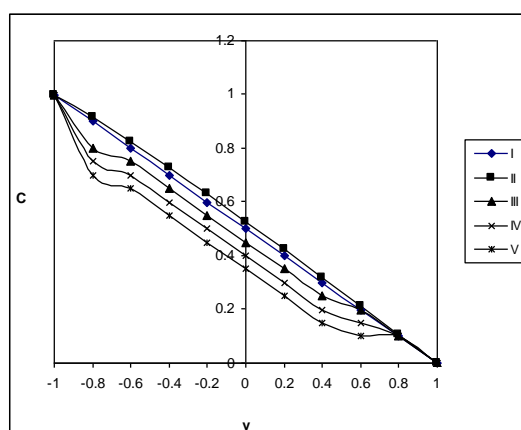


Fig. 16: Variation of C with N_1

	I	II	III	IV	V	VI
N_1	0.5	1.5	3.5	5	10	100

The non-dimensional concentration (C) is shown in figs (13-16) for a different parametric values. We find that the non-dimensional concentration is positive for all variations. This implies that the actual concentration is $> C_2$. The variation of C with M and m is shown in fig (13). It is found that higher the Lorentz force smaller the actual

concentration and for further higher Lorentz force larger the concentration in the flow region. Also it depreciates with $m \leq 1.5$ and enhances marginally with higher $m \geq 2.5$. When the molecular buoyancy force dominates over the thermal buoyancy force the actual concentration depreciates when the molecular buoyancy forces act in the same direction and for the forces acting in the opposite direction it enhances in the flow region. An increase in $\alpha \leq 4$ depreciates the actual concentration and enhances with higher $\alpha \geq 6$ (fig 14). The variation of C with Sc shows that lesser the molecular diffusivity smaller the actual concentration higher the constriction of the channel walls larger the actual concentration (fig 15). An increase in the radiation parameter $N_1 \leq 1.5$ enhances the actual concentration and it depreciates at $N_1 = 5$ and again enhances with higher $N_1 \geq 10$ (fig 16).

The rate of heat transfer (Nusselt Number) at the boundaries $\eta = \pm 1$ is shown in tables 1- 4 for different values of M , m , α , N , β , Sc , N_1 . It is found that the rate of heat transfer depreciates at $\eta = \pm 1$ with increase in $G > 0$ while an increase in $G < 0$ depreciates $|Nu|$ at $\eta = +1$ and enhances at $\eta = -1$. With respect to Hartmann number M we notice that higher the Lorentz force larger the rate of heat transfer at both the walls. An increase in the Hall Parameter $m \leq 1.5$ reduces $|Nu|$ and for higher $m \geq 2.5$ it enhances in the heating case and reduces in the cooling case at $\eta = +1$ while at $\eta = -1$ it depreciates in the heating case and enhances in the cooling case. The variation of Nu with heat source parameter α shows that the rate of heat transfer depreciates at $\eta = +1$ and enhances at $\eta = -1$ with increase in $\alpha \leq 4$ while for $\alpha \geq 6$ $|Nu|$ enhances at both the walls (Tables 1 & 3). The variation of Nu with buoyancy ratio N shows that when the molecular buoyancy force dominates over the thermal buoyancy force the rate of heat transfer enhances at $\eta = +1$ and reduces at $\eta = -1$ when the buoyancy forces act in the same direction and for the forces acting in opposite direction $|Nu|$ enhances at both the walls. The variation of Nu with the wavyness of the boundary β shows that higher the constriction of the channel walls smaller $|Nu|$ and for further higher constriction of the walls it enhances in the heating case and depreciates in the cooling case at $\eta = +1$ while at $\eta = -1$ smaller $|Nu|$ for all G . With respect to Schmidt Number Sc we find that lesser the molecular diffusivity larger $|Nu|$ at $\eta = +1$ and at $\eta = -1$ smaller $|Nu|$ and for further lowering of the diffusivity larger $|Nu|$ and for still lowering of the molecular diffusivity smaller $|Nu|$ (Tables 2 & 4). The variation of rate of heat transfer with thermal radiation parameter N_1 shows that at $\eta = +1$ the rate of heat transfer enhances with an increase in $N_1 \leq 1.5$ and for higher $N_1 = 10$ $|Nu|$ depreciates in the heating case and enhances in the cooling case and for still higher $N_1 = 100$, $|Nu|$ enhances for $G > 0$ and depreciates for $G < 0$. At $\eta = -1$ it enhances for $G > 0$ and depreciates for $G < 0$ with increase in $N_1 \leq 1.5$ and for higher $N_1 \geq 5$ it enhances for all G .

Table – 1
Nusselt number (Nu) at $y = +1$

G	I	II	III	IV	V	VI	VII	VIII	IX	X
10^3	-0.87111	0.31730	-0.06244	0.02270	0.04804	-0.01604	-0.50393	-0.87111	0.12598	-0.11838
3×10^3	0.17466	0.35083	0.56967	0.18425	0.19074	-0.44757	-1.97447	0.67466	2.03395	0.28455
-10^3	3.41725	-0.19145	-0.69832	2.42110	1.57507	-0.94939	0.68691	3.41725	3.34583	3.67270
-3×10^3	1.10663	0.95593	-0.88069	0.96752	0.78293	1.65302	2.70210	1.10663	1.49181	1.68514
M	2	4	10	2	2	2	2	2	2	2
m	0.5	0.5	0.5	1.5	2.5	0.5	0.5	0.5	0.5	0.5
α	2	2	2	2	2	4	6	2	2	2
N_1	0.5	0.5	0.5	0.5	0.5	0.5	0.5	1.5	5	10

Table – 2
Nusselt number (Nu) at $y = +1$

G	I	II	III	IV	V	VI	VII	VIII	IX	X
10^3	-0.87111	0.00250	0.00250	0.00250	-0.80298	0.12859	0.34432	0.00250	0.00450	-0.24301
3×10^3	0.17466	0.17466	0.17466	0.17466	-0.11153	0.31107	0.35973	0.17466	0.19466	0.27466
-10^3	3.41725	3.41725	3.41725	3.41725	-1.51666	0.95538	0.61010	3.41725	3.66725	3.96725
-3×10^3	1.10663	-0.88895	1.10663	1.10663	-45.98564	0.66770	0.51619	1.10663	1.46663	1.68663
N	1	2	-0.5	-0.8	1	1	1	1	1	1
β	-0.5	-0.5	-0.5	-0.5	-0.3	-0.7	-0.9	-0.5	-0.5	-0.5
Sc	1.3	1.3	1.3	1.3	1.3	1.3	1.3	0.24	0.6	2.01

Table – 3
Nusselt number (Nu) at $y = -1$

G	I	II	III	IV	V	VI	VII	VIII	IX	X
10^3	4.94340	-2.44455	9.26984	-2.86959	-2.63185	5.52801	17.59647	4.94340	-6.23763	-6.86523
3×10^3	-2.42677	-5.73812	9.20511	-2.36783	-2.23264	-4.50727	8.45554	-2.42677	-5.24731	-6.78120
-10^3	-1.09224	8.21377	8.70101	-1.16998	-1.24284	-3.72791	-7.07421	-1.09224	-2.77718	-3.56628
-3×10^3	-1.48436	9.52596	10.9648	-1.52629	-1.54284	-5.51270	-12.98062	-1.48436	-3.43804	-4.39151
M	2	4	10	2	2	2	2	2	2	2
m	0.5	0.5	0.5	1.5	2.5	0.5	0.5	0.5	0.5	0.5
α	2	2	2	2	2	4	6	2	2	2
N_1	0.5	0.5	0.5	0.5	0.5	0.5	0.5	1.5	5	10

Table – 4
Nusselt number (Nu) at $y = -1$

G	I	II	III	IV	V	VI	VII	VIII	IX	X
10^3	4.94340	-2.99987	-2.90987	-3.09987	18.66235	-3.76995	-1.46593	-2.99987	-2.69987	-9.79429
3×10^3	-2.42677	-2.20677	-2.02677	-2.72677	-5.09023	-1.42842	-0.84893	-2.42677	-2.32677	-2.40677
-10^3	-1.09224	-1.00224	-1.19224	-1.29224	-1.58686	-0.93451	-0.64344	-1.09224	-0.99224	-0.90224
-3×10^3	-1.48436	0.91010	-1.28436	-1.68436	-1.95902	-1.09427	-0.71157	-1.48436	-1.28436	-1.20436
N	1	2	-0.5	-0.8	1	1	1	1	1	1
β	-0.5	-0.5	-0.5	-0.5	-0.3	-0.7	-0.9	-0.5	-0.5	-0.5
Sc	1.3	1.3	1.3	1.3	1.3	1.3	1.3	0.24	0.6	2.01

Table – 5
Sherwood number (Sh) at $y = +1$

G	I	II	III	IV	V	VI	VII	VIII	IX	X
10^3	-0.06800	-6.09488	19.81663	-0.04221	-0.03796	-0.04361	-0.13128	-0.06800	-0.17072	-0.21378
3×10^3	-0.66155	-14.48638	17.88128	-0.43803	-0.22193	-0.44312	-0.48265	-0.66155	-1.12442	-1.33132
-10^3	0.01323	-6.89088	-6.48017	0.00106	-0.00791	-0.00838	0.01743	0.01323	0.04672	0.06206
-3×10^3	0.49240	-14.99488	2.47704	0.32885	0.16482	0.24317	0.32511	0.49240	0.77489	0.87914
M	2	4	10	2	2	2	2	2	2	2
m	0.5	0.5	0.5	1.5	2.5	0.5	0.5	0.5	0.5	0.5
α	2	2	2	2	2	4	6	2	2	2
N_1	0.5	0.5	0.5	0.5	0.5	0.5	0.5	1.5	5	10

Table – 6
Sherwood number (Sh) at $y = +1$

G	I	II	III	IV	V	VI	VII	VIII	IX	X
10^3	-0.06800	-0.10717	-0.10717	-0.12717	-0.95833	-0.01615	-0.00109	-0.50472	-0.20615	-0.07245
3×10^3	-0.66155	-0.86155	-0.66155	-0.68155	-3.98125	-0.14089	-0.02419	-4.05929	-1.47260	-0.42659
-10^3	0.01323	0.02323	0.01323	0.01623	0.13046	-0.01092	-0.00133	0.26134	0.08126	-0.00765
-3×10^3	0.49240	0.66241	0.49240	0.50240	1.97593	0.10848	0.01203	2.66044	1.10844	0.29914
N	1	2	-0.5	-0.8	1	1	1	1	1	1
β	-0.5	-0.5	-0.5	-0.5	-0.3	-0.7	-0.9	-0.5	-0.5	-0.5
Sc	1.3	1.3	1.3	1.3	1.3	1.3	1.3	0.24	0.6	2.01

The rate of mass transfer (Sherwood Number) at $\eta = \pm 1$ is exhibited in tables 5 – 8 for different parametric variations. The variation of Sh with Hartmann Number M shows that the rate of mass transfer at $\eta = +1$ enhances with increase in $M \leq 4$ and for higher $M = 6$ it enhances for $G > 0$ and depreciates for $G < 0$. At $\eta = -1$ the rate of mass transfer enhances with increase in M, an increase in the Hall parameter m depreciates the rate of mass transfer at $\eta = \pm 1$. An increase in the heat source parameter $\alpha \leq 4$ depreciates |Sh| at both the walls and for higher $\alpha \geq 6$ |Sh| enhances at $\eta = +1$ while at $\eta = -1$ it depreciates for $G > 0$ and enhances for $G < 0$ (Tables 5 & 7). When the molecular buoyancy force dominates over the thermal buoyancy force the rate of mass transfer enhances when the buoyancy force act in the same direction and for the forces acting in opposite direction it enhances at $\eta = +1$ and depreciates at $\eta = -1$. The variation of Sh with β shows that higher the constriction of the channel walls smaller the rate of mass transfer at $\eta = \pm 1$. With respect to Sc we find that lesser the molecular diffusivity smaller the rate of mass transfer at both the walls (Tables 6 & 8). With respect to radiation parameter N_1 we find that higher the thermal radiative heat flux smaller the rate of mass transfer and for further higher radiative heat flux ($N_1 \geq 5$) larger |Sh| at both the walls.

Table – 7
Sherwood number (Sh) at $y = -1$

G	I	II	III	IV	V	VI	VII	VIII	IX	X
10^3	-0.07695	3.99676	-7.48531	0.05993	0.02901	0.05838	-0.02486	-0.07695	0.16114	0.21548
3×10^3	0.63402	12.20613	-10.09949	0.41518	0.20507	0.23995	-0.04789	0.63402	0.97912	1.10963
-10^3	-0.06858	3.95274	9.68789	0.02407	0.01299	0.04293	0.13128	-0.00858	0.01049	0.01282
-3×10^3	-0.47640	12.29646	14.75980	-0.31356	-0.15160	-0.09899	0.10567	-0.47640	-0.66966	-0.72423
M	2	4	10	2	2	2	2	2	2	2
m	0.5	0.5	0.5	1.5	2.5	0.5	0.5	0.5	0.5	0.5
α	2	2	2	2	2	4	6	2	2	2
N_1	0.5	0.5	0.5	0.5	0.5	0.5	0.5	1.5	5	10

Table – 8
Sherwood number (Sh) at $y = -1$

G	I	II	III	IV	V	VI	VII	VIII	IX	X
10^3	-0.07695	0.09226	0.09226	0.06226	0.45844	0.00416	-0.00051	0.43503	0.17826	0.03604
3×10^3	0.63402	0.63402	0.63402	0.60402	3.82881	0.13565	0.02356	3.88878	1.41396	0.40768
-10^3	-0.00858	-0.00858	-0.00858	-0.00658	-0.11035	0.01023	0.01022	-0.22526	-0.06788	0.00978
-3×10^3	-0.47640	-85.85775	-0.47640	-0.27640	-1.91914	-0.10709	-0.01316	-2.57540	-1.07166	-0.28963
N	1	2	-0.5	-0.8	1	1	1	1	1	1
β	-0.5	-0.5	-0.5	-0.5	-0.3	-0.7	-0.9	-0.5	-0.5	-0.5
Sc	1.3	1.3	1.3	1.3	1.3	1.3	1.3	0.24	0.6	2.01

CONCLUSION :

Thus the magnetic field retards the magnitude of the axial velocity in the flow region. An increase in the Hall parameter m results an enhancement in the axial velocity. The variation of w with α shows that higher the strength of the heat generating sources smaller the velocity w in the entire flow region. The variation of w with β it is found that lesser the molecular diffusivity larger the velocity w also higher the constriction of the channel walls larger w in the region. Thus the wavyness of the boundaries results in an enhancement in the axial velocity. The effect of thermal radiation (N_1) on w ..

We find that lesser the molecular diffusivity smaller $|u|$ and for further lowering of the diffusivity larger $|u|$. The variation of u with β shows that higher the constriction of the channel walls larger $|u|$ in the entire flow region. We find that $|u|$ enhances with increase in the radiation parameter N_1 . Thus higher the radiative heat flux larger the magnitude of u in the flow region.

θ with Sc and β . The variation of θ with Sc shows that lesser the molecular diffusivity smaller the actual temperature in the entire flow region. With respect to β we notice that higher the constriction of the channel walls larger the actual temperature in the flow region. We find that higher the radiative heat flux lesser the actual temperature in the flow region.

Also it depreciates with $m \leq 1.5$ and enhances marginally with higher $m \geq 2.5$. When the molecular buoyancy force dominates over the thermal buoyancy force the actual concentration depreciates when the molecular buoyancy forces act in the same direction and for the forces acting in the opposite direction it enhances in the flow region. An increase in the radiation parameter $N_1 \leq 1.5$ enhances the actual concentration and it depreciates at $N_1 = 5$ and again enhances with higher $N_1 \geq 10$

The variation of Nu with the wavyness of the boundary β shows that higher the constriction of the channel walls smaller $|Nu|$ and for further higher constriction of the walls it enhances in the heating case and depreciates in the cooling case at $\eta = +1$ while at $\eta = -1$ smaller $|Nu|$ for all G . The variation of rate of heat transfer with thermal radiation parameter N_1 shows that at $\eta = +1$ the rate of heat transfer enhances with an increase in $N_1 \leq 1.5$ and for higher $N_1 = 10$

$|Nu|$ depreciates in the heating case and enhances in the cooling case and for still higher $N_1=100$, $|Nu|$ enhances for $G > 0$ and depreciates for $G < 0$. At $\eta = -1$ it enhances for $G > 0$ and depreciates for $G < 0$ with increase in $N_1 \leq 1.5$ and for higher $N_1 \geq 5$ it enhances for all G .

The variation of Sh with β shows that higher the constriction of the channel walls smaller the rate of mass transfer at $\eta = \pm 1$.

With respect to radiation parameter N_1 we find that higher the thermal radiative heat flux smaller the rate of mass transfer and for further higher radiative heat flux ($N_1 \geq 5$) larger $|Sh|$ at both the walls

REFERENCES:

1. N Ahmed and H.K. Sarmah : MHD Transient flow past an impulsively started infinite horizontal porous plate in a rotating system with hall current: *Int J. of Appl. Math and Mech.* 7(2) : 1-15, 2011.
2. M.M. Alam, and M.A. Sattar :Unsteady free convection and mass transfer flow in a rotating system with Hall currents,viscous dissipation and Joule heating, *Journal of Energy heat and mass transfer*,V.22,pp.31-39,2000
3. O, Anwar Beg, Joaquin Zueco and H.S. Takhar : Unsteady magneto-hydrodynamic Hartmann-Couette flow and heat transfer in a Darcian channel with hall currents, ionslip, Viscous and Joule heating : Network Numerical solutions, *Commun Nonlinear Sci Numer Simulat*,V.14,pp.1082-1097, 2009.
4. Cheng-Yang Cheng, Combined heat and mass transfer in natural convection flow from a vertical wavy surface in a power-law fluid saturated porous medium with thermal and mass stratification. *Int.Commun.Heat and Mass transfer* 36, 351-356, 2009
5. G, Comini., C.Nomino and S.Savino:Convective heat and mass transfer in wavy finned-tube exchangers.,*Int.J.Num.Methods for heat and fluid flow.*,V.12(6),pp.735-755, 2002.
6. L. Debnath : Exact solutions of unsteady hydrodynamic and hydromagnetic boundary layer equations in a rotating fluid system, *ZAMM*, V.55, p.431,1975
7. L. Debnath : *ZAMM*.V.59,pp.469-471, 1979
8. K.S. Deshikachar, and A. Ramachandra Rao : Effect of a magnetic field on the flow and blood oxygenation in channel of variables cross section , *Int.J.Engg. Sci*, V.23, p.1121, 1985.
9. Hyon Gook Wan, Sang Dong Hwang, Hyung He Cho : Flow and heat /mass transfer in a wavy duct with various corrugation angles in two-dimensional flow. *Heat and Mass transfer* ,V.45,pp.157-165, 2008
10. Jer-huan Jang and Wei-mon Yan:mixed convection heat and mass transfer along a vertical wavy surface,*Int.j.heat and mass transfer* ,v.47,i.3,pp.419-428, 2004

11. D.V. Krishna, D.R.V. Prasada Rao, A.S.Ramachandra Murty : Hydromagnetic convection flow through a porous medium in a rotating channel., *J.Engg. Phy. and Thermo. Phy*, V.75(2), pp.281-291, 2002
12. A. Mahdy, R.A. Mohamed and F.M.Hady : Natural Convection Heat and Mass Transfer over a vertical wavy surface with variable wall temperature and concentration in porous media: *Int.J. of Appl. Math and Mech.* 7(3): 1-13, 2011.
13. M. McMichael and S.Deutch : *Phys.Fluids*,V.27,p.110, 1984.
14. Naga Leela Kumari :Effect of Hall current on the convective heat and mass transfer flow of a viscous fluid in a horizontal channel, *Pesented at APSMS conference, SBIT, Khammam*, 2011
15. I. Pop,I : *J.Maths.Phys.Sci.*,V.5,p.375,1971
16. D.R.V.Rao, D.V.Krishna, and L.Debnath:Combined effect of free and forced convection on Mhd flow in a rotating porous channel,*Int.J.Maths and Math.Sci*,V.5,pp.165-182,1982
17. B.V. Rathish Kumar, Shalini Gupta. : Combined influence of mass and thermal stratification on double diffusion non-Darcian natural convection form a wavy vertical channel to porous media, *ASME J. Heat Transfer* 127,637-647, 2005
18. D.A.S. Rees, I. Pop. : A note on free convection along a vertical wavy surface in a porous medium. *ASME J. Heat Transfer* 116, 505-508, 1994
19. D.A.S. Rees, I.Pop : Free convection induced by a vertical wavy surface with uniform heat flux in a porous medium, *ASME J. Heat Transfer* 117, 547-550, 1995
20. D. Sarkar, S.Mukherjee : *Acta Ciencia Indica.*,V.34M,No.2,pp.737-751,2008
21. Sato,H:*J.Phy.Soc.,Japan*,V.16,p.1427,1961
22. G.S. Seth, S.Ansari, N.Mahto, S.K.Singh :*Acta ciencia Indica*, V.34M. No.3, pp.1279-1288, 2008.
23. B.V.Shalini, Rathish Kumar, Influence of variable heat flux on natural convection along a corrugated wall in porous media, *Commun.Nonlinear Sci.Numer. Simul.* 12, 1454-1463, 2007.
24. G.Shanti : Hall effects on convective heat and mass transfer flow of a viscous fluid in a vertical wavy channel with oscillatory flux and radiation,*J.Phys and Appl. Phya*, V.22, no.4, 2010
25. A. Sherman, and G.W.Sutton : Mhd ,Evanston,*Illionis*,p.173, 1961
26. R. Sivaprasad, D.R.V.Prasada Rao, and D.V. Krishna : Hall effects on unsteady Mhd free and forced convection flow in a porous rotating channel., *Ind.J. Pure and Appl.Maths*,V.19(2)pp.688-696, 1988
27. A. Sreeramachandra Murthy : Buoyancy induced hydromagnetic flows through a porous medium-A study ,Ph.D thesis, S.K.University, Anantapur, A.P, India, 1992

28. K. Vajravelu, and L. Debnath : Non-linear study of convective heat transfer and fluid flows induced by traveling thermal waves, *Acta Mech*, V.59, pp.233-249, 1986
29. K. Vajravelu and K.S. Sastry : forced convective heat transfer in a viscous incompressible fluid confined between a long vertical wavy wall and parallel flat wall, *J. fluid .Mech*, v.86(20), p.365, 1978
30. K. Vajravelu, and A.H. Neyfeh : Influence of wall waviness on friction and pressure drop in channels, *Int. J. Mech and Math. Sci.* V.4, N0.4, pp.805-818, 1981
31. T. Yamanishi : Hall effects on hydromagnetic flow between two parallel plates., *Phy. Soc., Japan, Osaka*, V.5, p.29, 1962